Supplementary Information

The role of Al-doping with different sites on structure and electrochemical performance of spherical $LiNi_{0.5}Mn_{1.5}O_4$ cathode materials for lithium-ion battery

Anyong Chen,‡ [a] Linglong Kong,‡ [b,c] Yang Shu,[c] Wenchao Yan,[b,c] Wei Wu,[b,c] Yongji Xu,*[a] Hongtao Gao*[a] and Yongcheng Jin*[b,c]

[a] *State Key Laboratory Base of Eco-Chemical Engineering, College of Chemistry and Molecular Engineering, Qingdao University of Science & Technology, Qingdao 266042, China.*
[b] *Center of Materials Science and Optoelectronics Engineering，University of Chinese Academy of Sciences, Beijing 100049, China.*
[c] *Qingdao Institute of Bioenergy and Bioprocess Technology, Chinese Academy of Sciences, Qingdao 266101, China.*
*corresponding authors
E-mail address：xuyj1960@126.com (Y. Xu), gaohtao@qust.edu.cn (H. Gao), jinyc@qibebt.ac.cn (Y. Jin)
‡ These authors contributed equally to this work.

Table S1 The ICP-AES results of the prepared LNMO samples.

	Li	Ni	Mn	Al
$LiNi_{0.5}Mn_{1.5}O_4$	1.01	0.49	1.49	0.00
$Li_{0.95}Ni_{0.45}Al_{0.05}Mn_{1.5}O_4$	0.98	0.44	1.49	0.047
$Li_{1.03}Ni_{0.5}Al_{0.03}Mn_{1.47}O_4$	1.05	0.51	1.46	0.028
$LiNi_{0.475}Al_{0.05}Mn_{1.475}O_4$	1.02	0.468	1.47	0.047

Table S2 Lattice parameters of LNMO cathode materials with Al-doping at different sites and various contents.

Sample	*a/nm*	*V/nm³*	I_{111}/I_{311}
$LiNi_{0.5}Mn_{1.5}O_4$	0.81715	0.54564	2.04
$Li_{0.99}Ni_{0.49}Al_{0.01}Mn_{1.5}O_4$	0.81697	0.54528	2.08
$Li_{0.97}Ni_{0.47}Al_{0.03}Mn_{1.5}O_4$	0.81693	0.54520	2.27
$Li_{0.95}Ni_{0.45}Al_{0.05}Mn_{1.5}O_4$	0.81684	0.54502	2.34
$Li_{0.97}Ni_{0.43}Al_{0.07}Mn_{1.5}O_4$	0.81675	0.54484	2.11
$Li_{1.01}Ni_{0.5}Al_{0.01}Mn_{1.49}O_4$	0.81679	0.54492	2.09
$Li_{1.03}Ni_{0.5}Al_{0.03}Mn_{1.47}O_4$	0.81681	0.54496	2.54
$Li_{1.05}Ni_{0.5}Al_{0.05}Mn_{1.45}O_4$	0.81682	0.54498	2.20
$Li_{1.07}Ni_{0.5}Al_{0.07}Mn_{1.43}O_4$	0.81686	0.54506	2.41
$LiNi_{0.495}Al_{0.01}Mn_{1.495}O_4$	0.81676	0.54486	2.04
$LiNi_{0.485}Al_{0.03}Mn_{1.485}O_4$	0.81661	0.54456	2.28
$LiNi_{0.475}Al_{0.05}Mn_{1.475}O_4$	0.81652	0.54438	2.28
$LiNi_{0.465}Al_{0.07}Mn_{1.465}O_4$	0.81643	0.54420	2.18
JCPDS (80-2162)	0.817	0.54534	2.66

Table S3 Structural parameters after Rietveld refinements.

$Li_{0.95}Ni_{0.45}Al_{0.05}Mn_{1.5}O_4$

($Fd\bar{3}m$, a = b = c = 8.1650 Å, α = β = γ = 90°, Rp=2.29, GOF=1.16, wRp=2.91.)

Atom	Wyckoff symbol	x	y	z	Uiso	Site occupancy
Li1	8a	0.500	0.500	0.500	0.042	0.886
Li2	16d	0.625	0.125	0.125	0.042	0.008
Mn1	16d	0.625	0.125	0.125	0.003	0.750
Al1	16d	0.625	0.125	0.125	0.012	0.025
Ni1	16d	0.625	0.125	0.125	0.003	0.217
Ni2	8a	0.500	0.500	0.500	0.003	0.017
O1	32e	0.635	0.365	0.135	0.015	1.000
Li2	16d	0.625	0.125	0.125	0.042	0.008
Mn1	16d	0.625	0.125	0.125	0.003	0.750

$Li_{1.03}Ni_{0.5}Al_{0.03}Mn_{1.47}O_4$

($Fd\bar{3}m$, a = b = c = 8.1666 Å, α = β = γ = 90o, Rp=2.23, GOF=1.22, wRp=2.90)

Atom	Wyckoff symbol	x	y	z	Uiso	Site occupancy
Li1	8a	0.500	0.500	0.500	0.038	1.000
Mn1	16d	0.625	0.125	0.125	0.009	0.735
Al1	16d	0.625	0.125	0.125	0.012	0.015
Ni1	16d	0.625	0.125	0.125	0.009	0.250
O1	32e	0.638	0.362	0.138	0.010	1.000

$LiNi_{0.475}Al_{0.05}Mn_{1.475}O_4$

($Fd\bar{3}m$, a = b = c = 8.1653 Å, α = β = γ = 90°, Rp=2.75, GOF=1.11, wRp=3.51)

Atom	Wyckoff symbol	x	y	z	Uiso	Site occupancy
Li1	8a	0.250	0.250	0.250	0.053	0.968
Li2	16d	0.625	0.125	0.125	0.053	0.016
Mn1	16d	0.625	0.125	0.125	0.007	0.738
Al1	16d	0.625	0.125	0.125	0.012	0.025
Ni1	16d	0.625	0.125	0.125	0.007	0.221
Ni2	8a	0.250	0.250	0.250	0.007	0.032
O1	32e	0.635	0.135	0.365	0.015	1.000

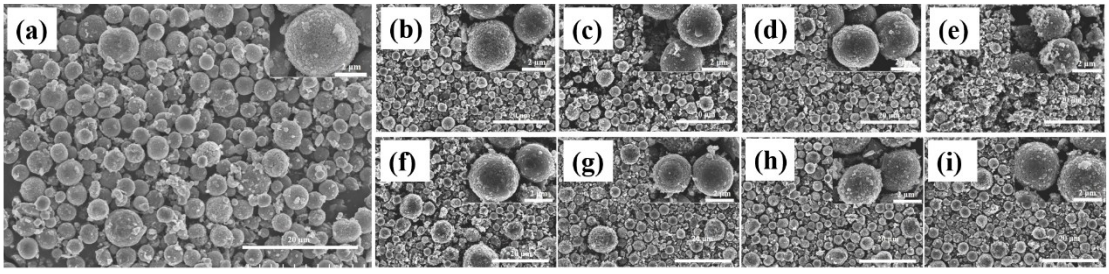

Fig. S1 SEM images of (a) $LiNi_{0.5}Mn_{1.5}O_4$, (b-e) $Li_{1-x}Ni_{0.5-x}Al_xMn_{1.5}O_4$ (x=0.01, 0.03, 0.05 and 0.07), and (f-i) $Li_{1+x}Ni_{0.5}Al_xMn_{1.5-x}O_4$ (x=0.01, 0.03, 0.05 and 0.07). The scale bar for the larger graphs is 20 μm, and the scale bar for the inserted graphs is 2μm.

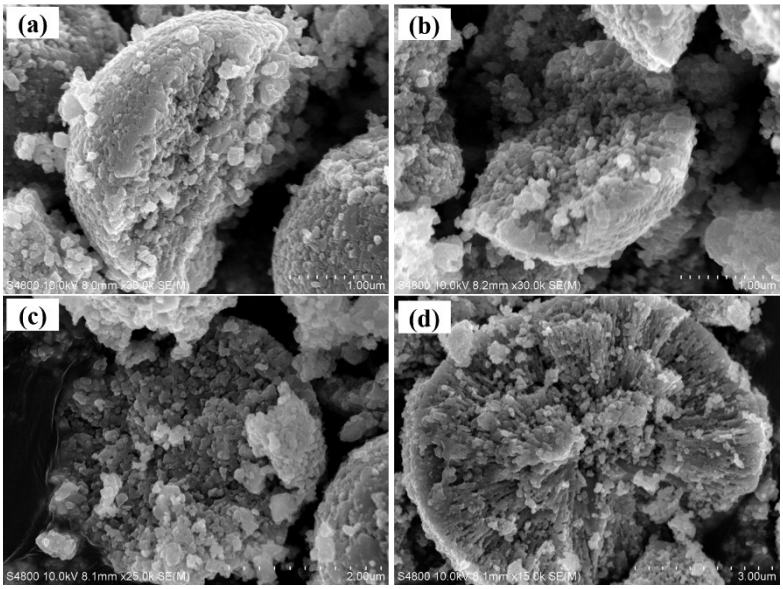

Fig. S2 Cross-sectional images of (a) $LiNi_{0.495}Al_{0.01}Mn_{1.495}O_4$ (x=0.01), (b) $LiNi_{0.485}Al_{0.03}Mn_{1.485}O_4$ (x=0.03), (c) $LiNi_{0.475}Al_{0.05}Mn_{1.475}O_4$ (x=0.05), and (d) $LiNi_{0.465}Al_{0.05}Mn_{1.465}O_4$ (x=0.07)

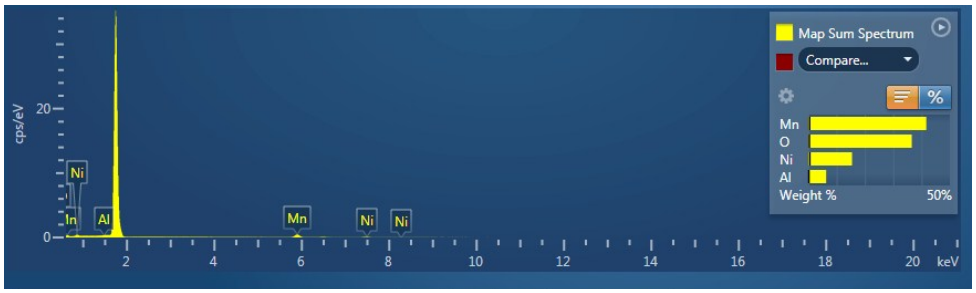

Fig. S3 Elemental map of $LiNi_{0.475}Al_{0.05}Mn_{1.475}O_4$ (x=0.05).

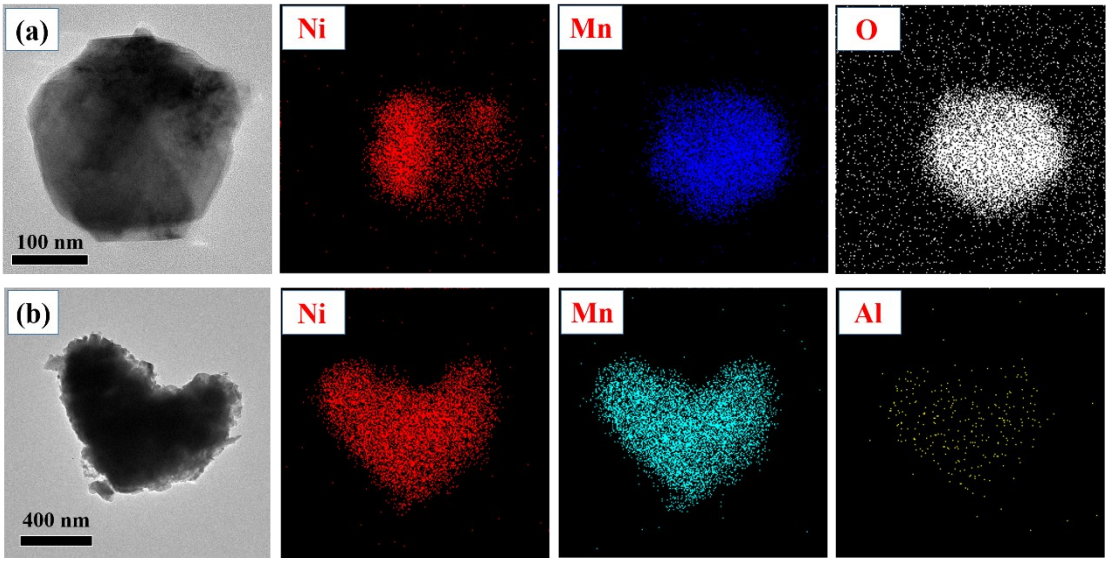

Fig. S4 TEM images of (a) $LiNi_{0.5}Mn_{1.5}O_4$ and (b) $LiNi_{0.475}Al_{0.05}Mn_{1.475}O_4$ combined with relevant elemental mappings of Ni, Mn, O, and Al.

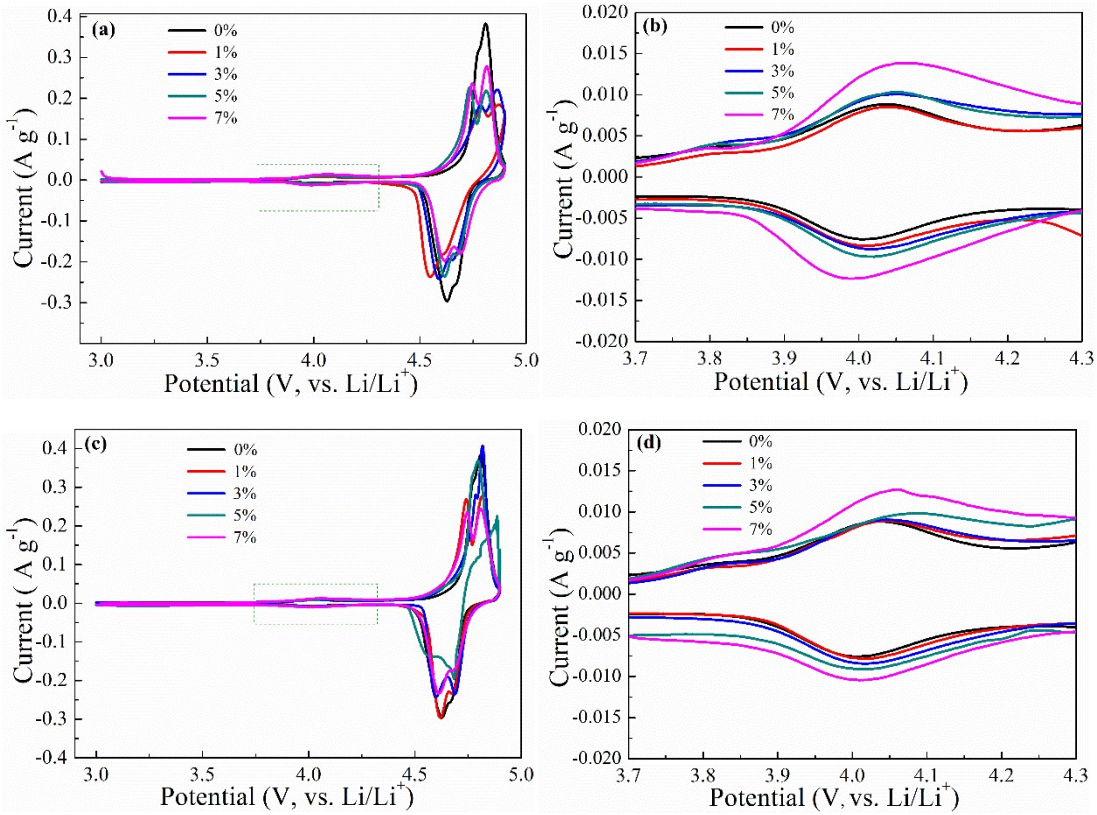

Fig. S5 Cyclic voltammetry curves of $Li_{1-x}Ni_{0.5-x}Al_xMn_{1.5}O_4$ (x=0, 0.01, 0.03, 0.05, and 0.07) (a) and $Li_{1+x}Ni_{0.5}Al_xMn_{1.5-x}O_4$ (x=0, 0.01, 0.03, 0.05, and 0.07) (c) combined with the relevant enlarged area (b) and (d) in the potential intervals of 3.7~4.3 V (vs. Li/Li^+).

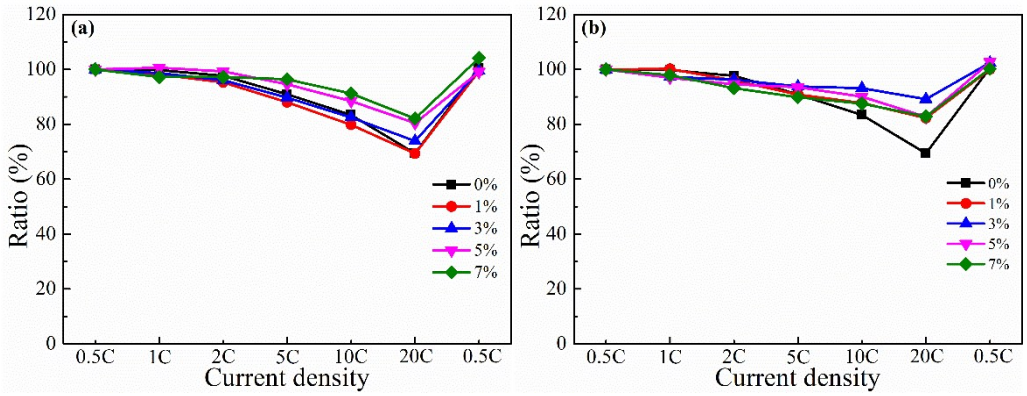

Fig. S6 Capacity ratios of (a) $Li_{1-x}Ni_{0.5-x}Al_xMn_{1.5}O_4$ and (b) $Li_{1+x}Ni_{0.5}Al_xMn_{1.5-x}O_4$ (x=0, 0.01, 0.03, 0.05, and 0.07) at various current densities (0.5 C, 1C, 2C, 5C, 10C and 20C).

Table S4 The specific capacities and capacity ratios of $Li_{1-x}Ni_{0.5-x}Al_xMn_{1.5}O_4$, $Li_{1+x}Ni_{0.5}Al_xMn_{1.5-x}O_4$, and $LiNi_{0.5-x/2}Al_xMn_{1.5-x/2}O_4$ (x=0, 0.01, 0.03, 0.05 and 0.07) at 55 °C (0.5C).

Sample	*1st cycle* *(mAh g-1)*	*50th cycle* *(mAh g-1)*	*Capacity ratio* *(%)*
$LiNi_{0.5}Mn_{1.5}O_4$	131	57.7	44.05
$Li_{0.99}Ni_{0.49}Al_{0.01}Mn_{1.5}O_4$	127.9	109.3	85.46
$Li_{0.97}Ni_{0.47}Al_{0.03}Mn_{1.5}O_4$	121.9	103.2	84.66
$Li_{0.95}Ni_{0.45}Al_{0.05}Mn_{1.5}O_4$	127.8	115.2	90.14
$Li_{0.97}Ni_{0.43}Al_{0.07}Mn_{1.5}O_4$	119.1	103.9	87.24
$Li_{1.01}Ni_{0.5}Al_{0.01}Mn_{1.49}O_4$	125.3	101.3	80.85
$Li_{1.03}Ni_{0.5}Al_{0.03}Mn_{1.47}O_4$	126.8	112.6	88.80
$Li_{1.05}Ni_{0.5}Al_{0.05}Mn_{1.45}O_4$	129.3	109	84.30
$Li_{1.07}Ni_{0.5}Al_{0.07}Mn_{1.43}O_4$	121	102	84.30
$LiNi_{0.495}Al_{0.01}Mn_{1.495}O_4$	124.6	96.3	77.29
$LiNi_{0.485}Al_{0.03}Mn_{1.485}O_4$	128.9	106.8	82.85
$LiNi_{0.475}Al_{0.05}Mn_{1.475}O_4$	126	111.7	88.65
$LiNi_{0.465}Al_{0.07}Mn_{1.465}O_4$	126.1	84.7	67.17

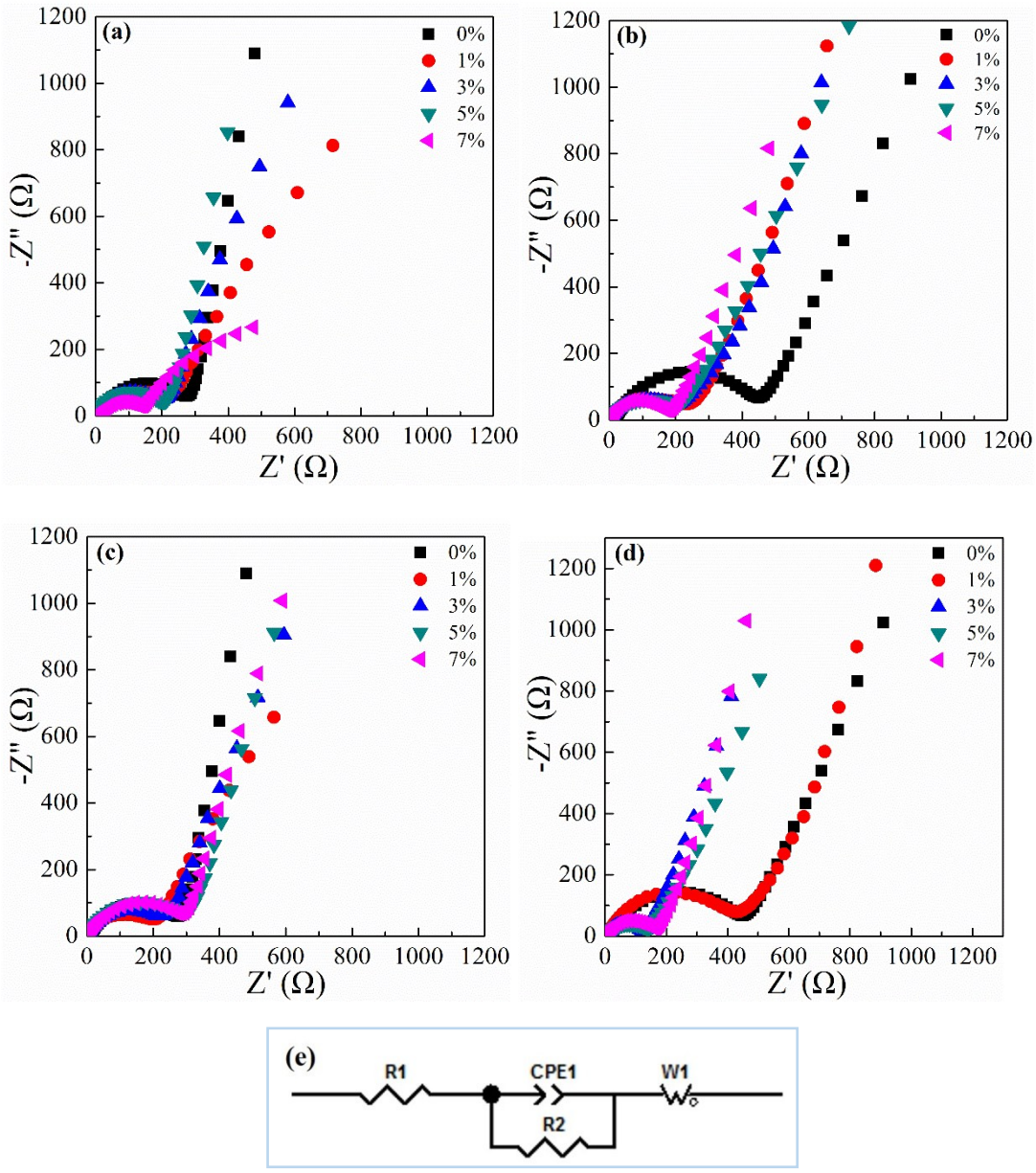

Fig. S7 EIS spectra of (a, b) $Li_{1-x}Ni_{0.5-x}Al_xMn_{1.5}O_4$ and (c, d) $Li_{1+x}Ni_{0.5}Al_xMn_{1.5-x}O_4$ (x=0, 0.01, 0.03, 0.05 and 0.07) before (a, c) and after 200 cycles (b, d) at 0.5C combining with the applied equivalent circuit (e). R_1 refers to the solution resistance, R_2 relates to the charge-transfer resistance, CPE_1 is the constant phase element, and W_1 donates the semi-infinite Warburg diffusion impedance.

Table S5 The stimulated values of R_2 before and after 200 cycles corresponding to the samples of $Li_{1-x}Ni_{0.5-x}Al_xMn_{1.5}O_4$, $Li_{1+x}Ni_{0.5}Al_xMn_{1.5-x}O_4$, and $LiNi_{0.5-x/2}Al_xMn_{1.5-x/2}O_4$ (x=0, 0.01, 0.03, 0.05 and 0.07) utilizing the equivalent circuit.

Sample	*R_2-0th cycle* *(Ω)*	*R_2-200th cycle* *(Ω)*	*ΔR_2* *(Ω)*
$LiNi_{0.5}Mn_{1.5}O_4$	232.6	400	167.4
$Li_{0.99}Ni_{0.49}Al_{0.01}Mn_{1.5}O_4$	218.7	200.3	-18.4
$Li_{0.97}Ni_{0.47}Al_{0.03}Mn_{1.5}O_4$	170.8	160.3	-10.5
$Li_{0.95}Ni_{0.45}Al_{0.05}Mn_{1.5}O_4$	175	158.5	-16.5
$Li_{0.97}Ni_{0.43}Al_{0.07}Mn_{1.5}O_4$	105.6	147.7	42.1
$Li_{1.01}Ni_{0.5}Al_{0.01}Mn_{1.49}O_4$	175.4	370.1	194.7
$Li_{1.03}Ni_{0.5}Al_{0.03}Mn_{1.47}O_4$	172.4	107.5	-64.9
$Li_{1.05}Ni_{0.5}Al_{0.05}Mn_{1.45}O_4$	250.9	112.7	-138.2
$Li_{1.07}Ni_{0.5}Al_{0.07}Mn_{1.43}O_4$	256.4	136.3	-120.1
$LiNi_{0.495}Al_{0.01}Mn_{1.495}O_4$	210.8	160.2	-50.6
$LiNi_{0.485}Al_{0.03}Mn_{1.485}O_4$	160.6	158.4	-2.2
$LiNi_{0.475}Al_{0.05}Mn_{1.475}O_4$	155	115.3	-39.7
$LiNi_{0.465}Al_{0.07}Mn_{1.465}O_4$	135.1	360.8	225.7

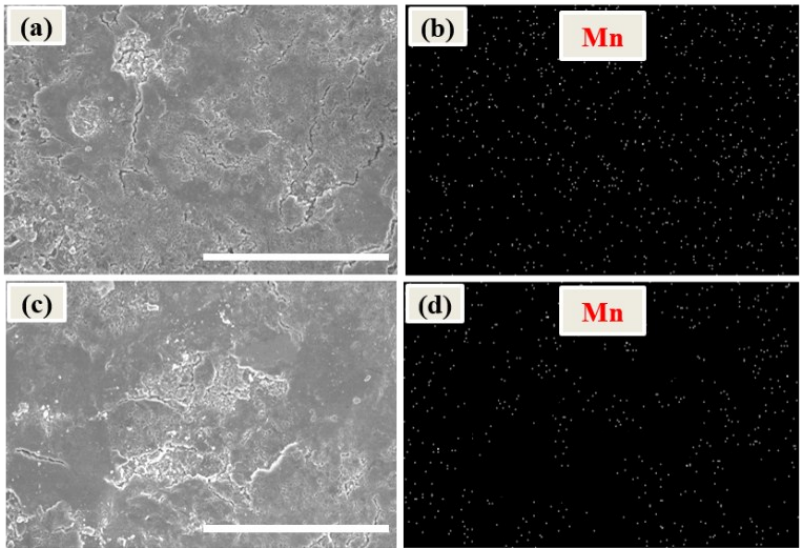

Fig. S8. SEM images of the cycled lithium anode in the $LiNi_{0.5}Mn_{1.5}O_4$ (a) and (c) $LiNi_{0.475}Al_{0.05}Mn_{1.475}O_4$ batteries systems combining with the distribution of Mn in the Li anode surface (b, d). The scale bar for (a) and (c) is 200 μm.

Table S6 The specific content values of Mn on the Li anode referring to $LiNi_{0.5}Mn_{1.5}O_4$ and $LiNi_{0.475}Al_{0.05}Mn_{1.475}O_4$ batteries systems from the EDS.

Sample	**Mn dissolution content (%)**
$LiNi_{0.5}Mn_{1.5}O_4$	0.52
$LiNi_{0.475}Al_{0.5}Mn_{1.475}O_4$	0.35